Available online at www.sciencedirect.com
SCIENCE DIRECT®
Applied Catalysis B: Environmental 58 (2005) 289–297
APPLIED CATALYSIS B: ENVIRONMENTAL
www.elsevier.com/locate/apcatb

Catalytic oxidation of naphthalene using a Pt/Al_2O_3 catalyst

Je-Lueng Shie[a], Ching-Yuan Chang[b,*], Jia-Hao Chen[b], Wen-Tien Tsai[c], Yi-Hung Chen[b], Chyow-San Chiou[a], Chiung-Fen Chang[d]

[a]*Department of Environmental Engineering, National I-Lan University, I-Lan 260, Taiwan*
[b]*Graduate Institute of Environmental Engineering, National Taiwan University, Taipei 106, Taiwan*
[c]*Department of Environmental Engineering and Health, Chia-Nan University of Pharmacy and Science, Tainan 717, Taiwan*
[d]*Department of Environmental Science, Tung-Hai University, Taichung 407, Taiwan*

Received 30 August 2004; received in revised form 15 November 2004; accepted 19 November 2004
Available online 29 January 2005

Abstract

Polycylic aromatic hydrocarbons (PAHs) are listed as carcinogenic and mutagenic priority pollutants, belonging to the environmental endocrine disrupters. Most PAHs in the environment stem from the atmospheric deposition and diesel emission. Consequently, the elimination of PAHs in the off-gases is one of the priority and emerging challenges. Catalytic oxidation has been widely used in the destruction of organic compounds due to its high efficiency (or conversion of reactants), its economic benefits and good applicability.

This study investigates the application of the catalytic oxidation using $Pt/\gamma\text{-}Al_2O_3$ catalysts to decompose PAHs and taking naphthalene (the simplest and least toxic PAH) as a target compound. It studies the relationships between conversion, operating parameters and relevant factors such as treatment temperatures, catalyst sizes and space velocities. Also, a related reaction kinetic expression is proposed to provide a simplified expression of the relevant kinetic parameters.

The results indicate that the $Pt/\gamma\text{-}Al_2O_3$ catalyst used accelerates the reaction rate of the decomposition of naphthalene and decreases the reaction temperature. A high conversion (over 95%) can be achieved at a moderate reaction temperature of 480 K and space velocity below 35,000 h^{-1}. Non-catalytic (thermal) oxidation achieves the same conversion at a temperature beyond 1000 K. The results also indicate that Rideal–Eley mechanism and Arrhenius equation can be reasonably applied to describe the data by using the pseudo-first-order reaction kinetic equation with activation energy of 149.97 kJ/mol and frequency factor equal to 3.26×10^{17} s^{-1}.

Keywords: Polycylic aromatic hydrocarbons; Catalytic oxidation; $Pt/\gamma\text{-}Al_2O_3$ catalyst

1. Introduction

Polycylic aromatic hydrocarbons (PAHs) are ubiquitous carcinogenic substances to which humans are exposed from the environment. They are listed as carcinogenic and mutagenic priority pollutants, belonging to the environmental endocrine disrupters. Most PAHs stem from the atmospheric deposition, diesel emission, cigarette smoke and, especially, in certain industrial workplaces [1]. Consequently, the elimination of PAHs from waste gas is one of the most emergent challenges. A few efforts had been put on reducing PAHs in the exhausts. Naphthalene (Nap) is the most volatile member of this class of pollutants [2]. It poses a great ecotoxicological problem. Significant carcinogenic effects have been associated with Nap exposure in animal investigations. In 2000, the US National Toxicology Program (USNTP) revealed the clear evidence of the carcinogenic activity of Nap in rats [3]. Further, the European Union (EU) is currently preparing a new risk assessment report.

Nap is a constituent of diesel and jet fuel [4]. It is ubiquitously discharged into the human environment by incomplete combustion processes from industrial, domestic and natural sources (residential heating with fossil fuels, industrial plants, motor vehicle traffic, air traffic, gasoline burning, cigarette smoke, forest fires, etc.) [2]. The major exhausts of the diesel vehicles are particulates and PAHs,

* Corresponding author. Tel.: +886 2 2363 8994; fax: +886 2 2363 8994.
E-mail address: cychang3@ntu.edu.tw (C.-Y. Chang).

0926-3373/$ – see front matter © 2004 Elsevier B.V. All rights reserved.
doi:10.1016/j.apcatb.2004.11.026

which are emitted from diesel engines and can be much higher than those of Otto engines [5]. The control of particulars emitted from diesel engines has been studied for decades [6–8]. A few studies had examined the catalytic oxidation of PAHs. Li et al. [9] and Siegl et al. [10] pointed out that PAHs in diesel emissions mainly consisted of two to five aromatic rings, especially, Nap, phenanthrene and pyrene/fluoranthene. Li and Westerholm [11] found that two types on nitro-PAHs, nitropyrene and nitroperylene, emitted in diesel exhausts. Nitro-PAHs were reported to be more mutagenic and carcinogenic than PAHs due to the effects of the nitro group on metabolism processes [12]. The industrial production of Nap is predominantly based on the crystallization and distillation of coal tar, which is condensed and separated from coke oven gases. Although the industrial production of Nap and its application as an intermediate can contribute to the environmental Nap burden, it is widely accepted that the major part comes from burning processes (residential, industrial and natural sources). Most of the Nap released into the environment is attributable to the atmosphere (90%), with a small portion into water (5%) and soil (3%) [4]. Nap consists of a basic aromatic structure and is the simplest and least toxic PAH. Therefore, this study takes Nap as a target compound for the development of an abatement technique of PAHs emitted into the atmosphere: information obtained for Nap can enhance destruction technology for other PAHs.

Common methods applicable for eliminating Nap from the waste stream include biodegradation [13], absorption [14], adsorption [15], high-energy electron beam [16], ozonization [17,18] and catalytic oxidation [19–21]. Among them, the catalytic oxidation has been demonstrated as one of the cost-effective and efficient technologies to destroy the troublesome VOCs. Zhang et al. [19] investigated the activities of six metal catalysts (1% Pt, 1% Pd, 1% Ru, 5% Co, 5% Mo and 5% W on γ-Al_2O_3 support) in decomposing naphthalene at an O_2 concentration of 10 vol.%. For the utilization of biomass as a renewable energy resource, Li and Chen [20] studied the influence of Pt on the catalytic activity of Ni/Al_2O_3 in steam reforming by using naphthalene as a model compound. The reaction kinetics were also discussed. Neyestanaki and Lindfors [21] prepared a knitted silica-fibre and used it as support of catalysts for combustion. They also prepared different Pd-MeO and Pt-MeO (Me = Ni, Co, Cu and Mn) catalysts and investigated their catalytic activities in the conversion of gas mixtures consisting of methane, ethene, naphthalene (model PAH), carbon monoxide, carbon dioxide, nitrogen and water vapour in the temperature range of 423–1073 K to simulate the exhausts from stationary diesel engines. There are other catalysts, which have been utilized to oxidize PAHs, covering chlorinated and non-chlorinated VOCs, such as Pt/Al-MCM-41 [22], V_2O_5-WO_3/TiO_2 [23–26], Fe_2O_3 and MoO_3-V_2O_5 [27], Pd-Ce/Al_2O_3 [28], Pd-Ba/Al_2O_3 [29] and Pd-Zr/Y zeolite [30]. Anderson and Spivey [31] pointed out that the catalytic ability of oxidation of methane by using various catalysts on Al_2O_3 support are in the order of Pt > Pd > Mn > Cu. Heyes et al. [32] employed a series of catalysts to evaluate the destructive oxidation of *n*-butanal and methyl mercaptan. Their results indicated that the ability to destroy *n*-butanal in mixtures with methyl mercaptan at the end of life-tests, decreased in the order of CuO = Pt > MnO_2 > V_2O_5 > CO_3O_4. However, to the best of our knowledge, the reaction kinetics of the combustion of Nap over Pt/γ-Al_2O_3 catalyst has not been reported. The relationships between conversion efficiency, operating parameters and relevant factors such as treatment temperatures, catalyst sizes and space velocities are therefore examined in this study. Also, a related reaction kinetic expression is proposed to give a simplified expression of the relevant kinetic parameters.

2. Experimental

2.1. Materials

The solid naphthalene used is a product of Merck Chemical Inc. (purity > 99%). The commercial catalyst of DASH-220N employed was obtained from N.E. Chemcat Co. (Japan). The catalyst consists of 0.23 wt.% Pt (1.8 g/l) supported on γ-Al_2O_3 with the bulk density of 770 g/l. The Pt uniformly covers the γ-Al_2O_3 support with a value of Pt/BET surface area in 1 g catalyst of 1.38×10^{-3} g/(g m^2). Its basic properties are listed in Table 1. The DASH-220N catalyst used in this study is different from DASH-220 employed in a previous study [33], e.g., in Pt content. Adsorption and desorption isotherms of N_2 on uncrushed catalyst and catalyst of mesh size (ASTM) of 40–50 are shown in Figs. 1 and 2, respectively. The property of the pore type of DASH-220N is wide-mouth and its hysteresis loop is classified into type B [34]. From Figs. 1 and 2, the pore type has not changed after crushing. The catalyst was ground and sieved to 20–30 (0.59–0.84 mm), 40–50 (0.297–0.42 mm) and 50–60 (0.25–0.297 mm) ASTM mesh to examine and distinguish the intra-particle pore diffusion resistance. The scanning electron microscope (SEM, Hitachi S-2500) spectra were taken for the catalyst samples and are illustrated for mesh size 40–50 in Figs. 3 and 4. The catalyst consists of large pores constructed by plate structures.

2.2. Equipment, procedures and catalytic reactor

A schematic diagram of the fixed-bed catalytic reaction system is shown in Fig. 5. The system can be divided into three parts: (1) a feed gas sub-system, (2) a catalytic oxidation sub-system and (3) a combustion gas analyzing sub-system. The effluent gas simulation sub-system is composed of an air cylinder (20.95 vol.% O_2, Ching-Feng-Harng Co. Ltd.), a molecular sieve column (Super Chroma Enterprice Ltd.), a mass flow meter (Teledyne Hasting-Raydist, HFC-202B), two conditioning bottles (Pyrex), a heating tape (Electrothermal, HT 352) and a Nap vapor

Table 1
Physical characteristics and BET characterisation of Pt/γ-Al_2O_3 catalyst used in this study

Item	Specification	Measured or range selected
Pt/BET surface area in 1 g catalyst (g/(g m^2))	1.38×10^{-3}	–
Pt content (wt.%)	0.23 ± 0.02	0.23
Bulk density (g/l)	710–770	770
Moisture (%)	Maximum 2.00	0.78
Activity[a] (%)	Minimum 90	96
Carrier	Alumina sphere	–
Particle size (mm)	–	2–4
Total surface area[b] (m^2/g)	–	166.62
Total pore volume[c] (cm^3/g)	–	0.4392
Average pore diameter[b] (Å)	–	76.12
True density[d] (He displacement method) (g/cm^3)	–	3.22
Porosity[e]	–	0.59

[a] The value of activity (A) is calculated from the conversion of n-hexane with inlet concentration of 340 ppmv and inlet temperature of 200 °C. The inlet and outlet flows were measured by GC (air: 10 l/min; space velocity (SV): 1000 h^{-1}). A (%) = (1 − (outflow concentration/inflow concentration)) × 100.
[b] Brunauer, Emmett and Teller (BET) surface area and true density were measured by surface area analyzer (Micromerities Inc.; Model ASAP 2010) and pycnometer (AccuPyc 1330), respectively.
[c] Measured for total pore volume of pores in the ranges of 1.7–300 nm.
[d] Estimated by BET surface area and total pore volume.
[e] Computed from true density and total pore volume.

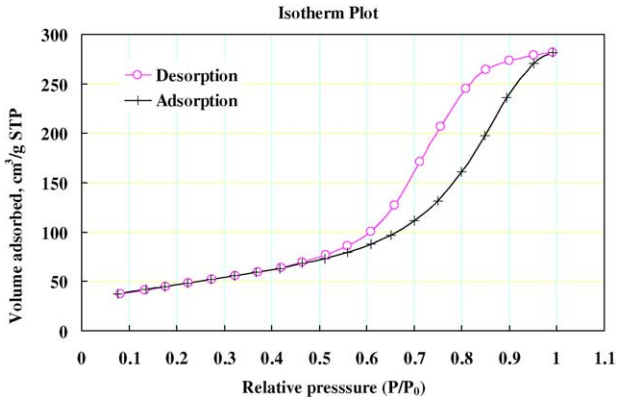

Fig. 1. Adsorption and desorption isotherms of N_2 on uncrushed Pt/γ-Al_2O_3 catalyst at 77 K.

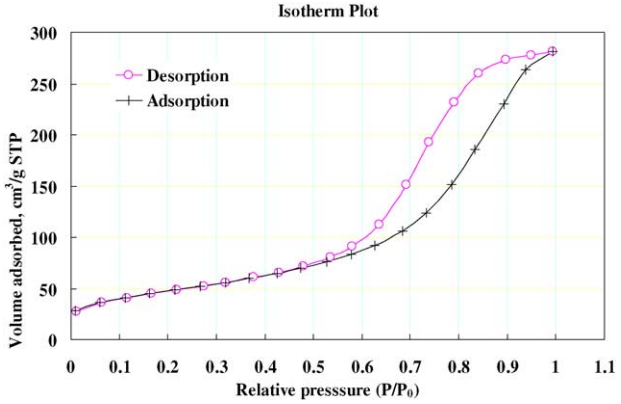

Fig. 2. Adsorption and desorption isotherms of N_2 on Pt/γ-Al_2O_3 catalyst with ASTM mesh size of 40–50 (0.297–0.42 mm) at 77 K.

generator (Pyrex). The material of piping, valves, regulators or fittings used are either SST-316 or Teflon. Oil-free air was dried by silica gel in a molecular sieve column. The dried air was metered to the system using a mass flow controller of 200 cm^3/min. It then passed through two conditioning bottles to buffer the air flow followed by one bottle full of solid Nap to generate Nap vapor. The temperature of the second Nap vapor generator was controlled at 323 K with a heating tape to provide a constant Nap vapor concentration of 600 ppmv. Connections between the Nap vapor generator and the heating furnace were kept at 373 K to prevent undesired condensation of Nap before combustion.

The catalytic incineration sub-system is composed of a tubular fixed-bed reactor (quartz), an electrical heating

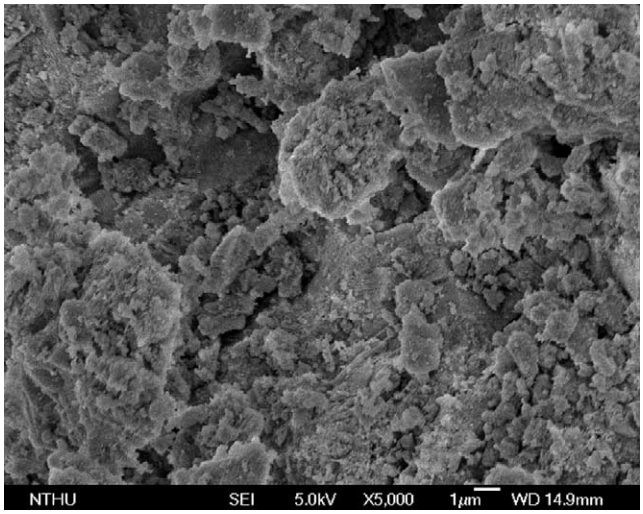

Fig. 3. SEM—micrography of Pt/γ-Al_2O_3 catalyst with mesh size of 40–50. Scale: ×5000.

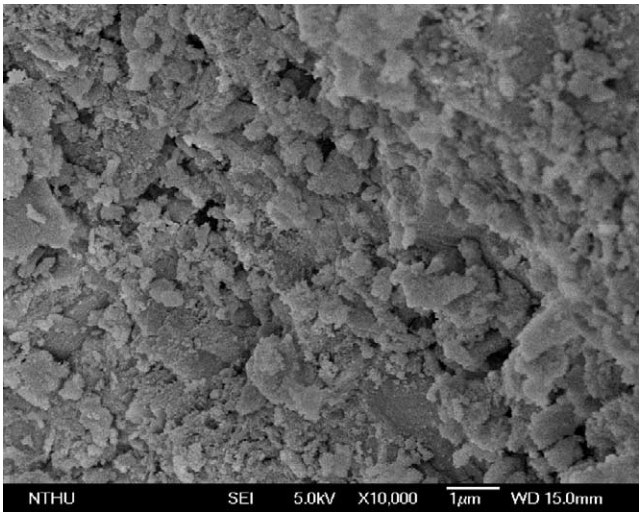

Fig. 4. SEM—micrography of Pt/γ-Al_2O_3 catalyst with mesh size of 40–50. Scale: ×10,000.

furnace (San-Ja Electric and Machinery Ltd.), a proportional integral derivative (PID) controller (Eurothem Co., H720), two chromel–alumel (K-type) thermocouples and one data acquisition system (Karma Technology Ltd., PICO, TC-08 (eight channel), Labview 5.0 (software)). The tubular fixed-bed reactor was housed in the middle section of the electrical heating furnace of 5 cm diameter and 40 cm length, to ensure uniform heating of the catalyst bed. The temperature of the reactor was controlled by the PID controller to maintain a stable temperature in the catalyst bed to within ±1 K of the set-point value. The length, internal and outer diameters of the reactor are 52, 1 and 1.2 cm, respectively.

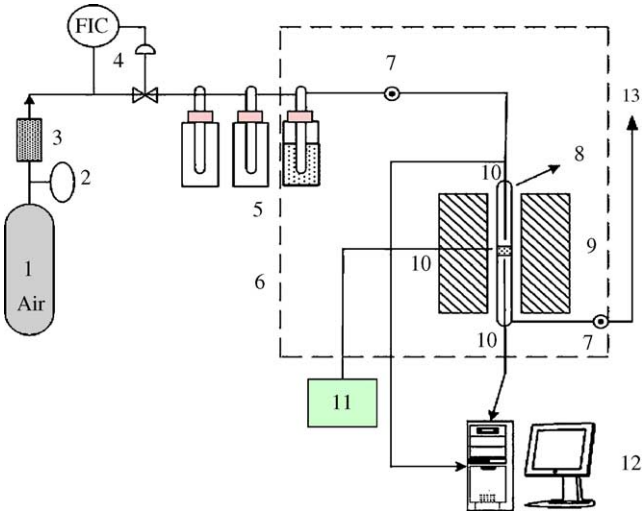

Fig. 5. Schematic layout for the catalytic decomposition of naphthalene (Nap). Components: (1) air cylinder, (2) regulation value, (3) molecular sieve column, (4) mass flow controller, (5) naphthalene generator, (6) heated components by electric tape, (7) sampling ports (to GC), (8) tubular fixed-bed reactor, (9) heating furnace, (10) thermocouple, (11) temperature controller, (12) data acquisition system and (13) vent to atmosphere.

A porous quartz disc was fixed in the middle of the reactor, 24 cm below its top, to support two layers of glass beads, two layers of quartz cotton and one layer of catalyst. The top and bottom layers of glass beads (3 mm diameter) and quartz cotton covered and supported the layer of catalyst serving as a zone for preheating and gas distribution for the inlet gas and as a zone for minimizing the axial mass and temperature gradient for the outlet gas, respectively. Two K-type thermocouples were inserted into the reactor, one from the top and the other from the bottom. The temperatures were measured 5 mm above and below the center of the catalyst packing. The temperature specified in this study is the average of the measured temperatures above and below.

2.3. Analytical methods

The gas analyzing sub-system is composed of a GC-FID (Hewlett Packard Inc., HP 5890 series II) and GC-TCD (China Chromatography, 8900). The GC-FID was used for the quantitative analyses of Nap vapor and hydrocarbon (HC) gaseous products. The chromatographic column of the GC-FID is a Zebron capillary GC column (Zebron ZB-1, 30 m long, 0.53 mm i.d., 1.5 μm film thickness). Integrating software (ChromManager Multisystem) from the Analytical Based Development Center (ABDC, Taiwan) was used in the computer for graphing and integrating purposes. The operating conditions of the GC-FID were set as follows: injector temperature 373 K, detector temperature 383 K, column temperature (following the sampling injection) being held at 373 K, nitrogen carrier gas flow rate 3.2 ml/min, nitrogen make-up gas 24 ml/min and sample volume 200 μl. For the analysis of non-hydrocarbon gases (e.g., H_2, CO, CO_2, O_2, N_2), a GC-TCD with a Supelco packing column (60/80 carbonxen-1000, 15 ft long, 2.1 mm i.d.) was used. The operation conditions were set as follows: injector temperature 373 K, detector temperature 373 K, column temperature (following the sampling injection) being held at 373 K for 30 min, helium carrier gas flow rate 35 ml/min for A and B columns, sample volume 800 μl. The principal standard gases are 99.9999% N_2, 99.9% CO_2, CO and H_2. The standard Nap concentrations for establishing the calibration curve were prepared by dissolving 1 g solid Nap into 20 ml butanol and then purging the solution with various volumes into a gas bag.

Quantitative analysis of gaseous products was conducted using the linear calibration response equations of standards. The equation was generated for each compound of gas standard using a minimum of five different concentrations with three replicates at each concentration. All correlation coefficients (R^2) of linear calibration response curves exceed 99.7%.

2.4. Experimental conditions

Purged air carried the vaporized Nap to simulate the waste gas from atmospheric diffusion and exhaust from

diesel engines. The simulated gas was injected into the catalytic reactor heated to the setting temperature by the electrical furnace. The concentration of Nap generated from the source reached steady state after an hour at 323 K. A given volume of gas samples was taken before and after the reaction, and injected into the GC to determine the concentration (C) and the conversion. Reaction studies were performed in the temperature range of 398–1150 K. Space velocities (SV), defined as the volumetric flow rate of feed divided by the catalyst volume, were varied in the range of 15,000 (1.1021 g of catalyst) to 100,000 h^{-1} (0.1567 g of catalyst). The reciprocal of SV represents the space time or the contact time between the target component and the catalyst. Process conditions were steadily maintained in order to assure the steady state within 5% relative error. Conversion and destruction efficiency of Nap (X, $X = (C_{in} - C_{out})/C_{in}$) was determined from the concentrations of the feed (C_{in}) and effluent (C_{out}) streams measured by GC analysis. Duplicate or triplicate runs were performed for each experimental case and the data presented are the average values. The concentrations of Nap and O_2 were 600 ppmv and 20.95 vol.%, respectively.

3. Results and discussion

3.1. Decomposition of naphthalene with and without Pt/γ-Al_2O_3

Fig. 6 shows the plots of the thermal decomposition of Nap both without catalyst at a space velocity of 15,000, 35,000 and 50,000 h^{-1} and with the commercial Pt/γ-Al_2O_3 catalyst at SV of 35,000 h^{-1}. The results indicate that the Pt/γ-Al_2O_3 catalyst used enhances the decomposition of Nap, significantly decreasing the required reaction temperature. A high conversion (over 95%) can be achieved at the moderate reaction temperature of 480 K and space velocity below 35,000 h^{-1}. At the same operation conditions, the reaction temperature needed to be as high as 1000 K to achieve the same conversion in the case without Pt/γ-Al_2O_3 catalyst.

Table 2 compares the temperatures of incineration of Nap at various conversions of 10 ($X_{10\%}$), 50 ($X_{50\%}$) and 90% ($X_{90\%}$). The results show that the thermal reaction without and with catalyst occurs at 962 and 442 K, 982 and 458 K, and 1123 and 475 K at the $X_{10\%}$, $X_{50\%}$ and $X_{90\%}$, respectively. This suggests that the use of catalyst of Pt/γ-Al_2O_3 is beneficial to the conversion of Nap.

Comparison of temperatures of oxidation of Nap at conversions of 10, 50 and 90% over Pt catalyst in this study and literatures [21,35–38] is also shown in Table 2, indicating that lower temperatures at $X_{10\%}$, $X_{50\%}$ and $X_{90\%}$ were achieved in this study. These results support the use of the catalytic oxidation system introduced in this study. It is noteworthy that the effect of the space velocity on the thermal decomposition of Nap without Pt/γ-Al_2O_3 catalyst is not obvious. The reason may be due to that the blank tests replaced catalyst packing by glass beads and varying space velocities using various volumes of glass beads is not the most suitable method to reflect the difference of reaction times. In a further kinetic study, the flow rate will be changed with a constant volume of glass beads.

3.2. Effects of operating parameters on naphthalene catalytic oxidation

In order to ensure the elimination of mass transfer effects, a series of tests were performed to examine the conversions of Nap over Pt/γ-Al_2O_3 catalyst with three particle sizes of mesh no. 20–30, 40–50 and 50–60. Fig. 7 shows that the differences in conversions are not significant. For convenience, catalyst of 40–50 mesh was employed to carry out the experiments for this study eliminating mass transfer effects. Fig. 8 presents the conversion as a function of reaction temperature at space velocities of 15,000, 25,000,

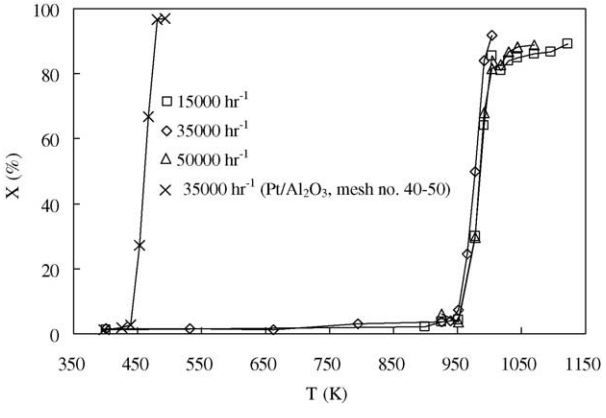

Fig. 6. Plots of the thermal decomposition of Nap via thermal oxidation (without catalyst) (□, ◇, △) and with Pt/γ-Al_2O_3 catalyst (×). □, ◇, △, ×: spacial velocity (SV) = 15,000, 35,000, 50,000 and 35,000 h^{-1}. Initial concentration of Nap (C_0) = 600 ppmv.

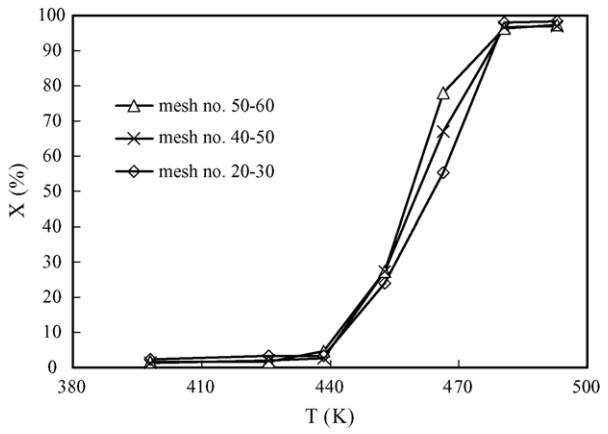

Fig. 7. Effect of temperature (T) on conversion (X) of Nap via oxidation at various catalyst sizes. C_0 = 600 ppmv and SV = 35,000 h^{-1}. △, □, ◇: mesh no. 50–60, 40–50 and 20–30.

Table 2
Comparison of temperatures of oxidation of naphthalene over Pt catalyst at various conversions of 10, 50 and 90% in this study and literatures

SV (h^{-1})	25,000			35,000		50,000	
	$T_{10\%}$ (K)[a]	$T_{50\%}$ (K)[b]	$T_{90\%}$ (K)[c]	$T_{50\%}$ (K)[b]	$T_{90\%}$ (K)[c]	$T_{50\%}$ (K)[b]	$T_{90\%}$ (K)[c]
In this study[d]	442	458	475	460	476	469	485
Blank test in this study	962[e]	982[e]	1123[e]	978	1003	983	1070
Carnö et al. [36][f]	467[g]	477[g]	583[g]	–	–	448	923
Neyestanaki and Lindfors [21][h]	459[g]	482[g]	506[g]	–	–	–	–
Ferrandon et al. [37][i]		543[j]					
Zhang et al. [19][k]	467[g]	–	476[g]	–	–	–	–

[a] $T_{10\%}$: temperature at 10% conversion of Nap.
[b] $T_{50\%}$: temperature at 50% conversion of Nap.
[c] $T_{90\%}$: temperature at 90% conversion of Nap.
[d] Experimental conditions: 600 ppmv Nap, 20.95 vol.% O_2, 0.23 wt.% Pt/γ-Al_2O_3 (commercial catalyst, DASH-220N).
[e] Spacial velocity (SV) = 15,000 h^{-1} without catalyst.
[f] Mixture of gas (50 ppmv Nap, 200 ppmv CH_4, 2550 ppmv CO, 12 vol.% CO_2, 10 vol.% O_2, 0–20 vol.% H_2O); 0.12 wt.% Pt/Al_2O_3 (commercial catalyst, NX-45).
[g] SV = 20,000 h^{-1}.
[h] Mixture of gas (50 ppmv Nap, 200 ppmv CH_4, 2500 ppmv CO, 12 vol.% CO_2, 10 vol.% O_2, 12 vol.% H_2O); 0.3 wt.% Pt/silica-fibre.
[i] Mixture of gas (50 ppmv Nap, 200 ppmv CH_4, 2550 ppmv CO, 12 vol.% CO_2, 10 vol.% O_2, 13.5 vol.% H_2O).
[j] 0.05 mol% Pt/γ-Al_2O_3; SV = 23,000 h^{-1}.
[k] 100 ppmv Nap, 10 vol.% O_2; 1 wt.% Pt/γ-Al_2O_3.

35,000, 50,000 and 10,000 h^{-1} for the incineration of Nap over Pt/γ-Al_2O_3 catalyst. All results were obtained at the same Nap inlet concentration of 600 ppmv. The Nap can be destroyed with efficiencies in excess of 90% when it is catalytically oxidized at 485 K with space velocity below 50,000 h^{-1}. The lower the space velocity (the higher the contact time), the higher is the conversion of Nap at the same temperature, being consistent with that of the oxidation of other VOCs reported previously [33]. Zhang et al. [19] pointed out that the reaction of Nap via oxidation over Pt/γ-Al_2O_3 catalyst became insensitive to the concentration of oxygen once the reaction temperature exceeded 413 K, the reason being that chemisorption of oxygen appeared to be the rate-determining step at a reaction temperature below 413 K. Note that Everaert and Baeyens [25] indicated that the oxygen-concentration can be of importance if below 3 vol.% and it was clear that the rate of reaction was of zero-order with respect to O_2 concentration above 3 vol.%. In this study, the starting temperatures were all above 413 K. It is hence reasonable to assume that the concentration of oxygen does not affect the reaction rate of catalytic oxidation of Nap. Hence, air was chosen as carrier gas to carry out the experiments.

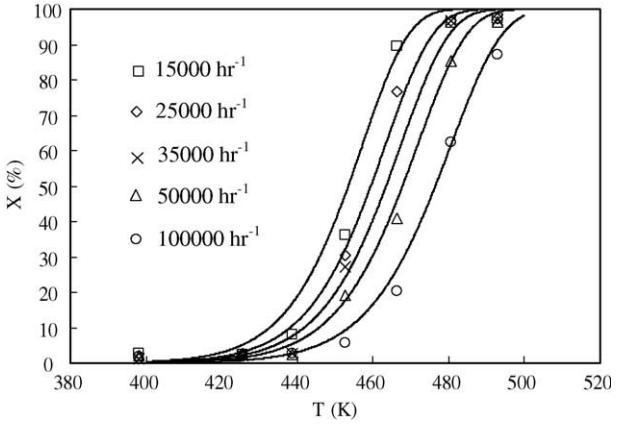

Fig. 8. Effects of T on X of Nap via oxidation using Pt/γ-Al_2O_3 catalyst with mesh size of 40–50 at various space velocities. C_0 = 600 ppmv. □, ◇, ×, △, ○: SV = 15,000, 25,000, 35,000, 50,000 and 100,000 h^{-1}. Line: computed by a best fit. Symbol: experimental.

3.3. Incineration products of naphthalene over Pt/γ-Al_2O_3

In order to compute the level of completeness of reaction of Nap via catalytic oxidation, we introduce an index of mineralization ($M = [CO_2]_e/[CO_2]_t \times 100$, %). The $[CO_2]_e$ and $[CO_2]_t$ denote the CO_2 concentration measured and that theoretically produced by complete incineration of Nap ($C_{10}H_8 + 12O_2 \rightarrow 10CO_2 + 4H_2O$), respectively: M therefore represents the amount of CO_2 produced during catalytic oxidation relative to the maximum amount of CO_2 resulting

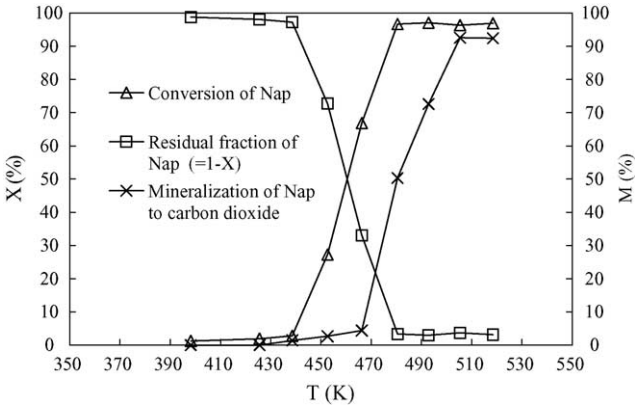

Fig. 9. Plots of X, residual fraction and mineralization (M) of Nap using Pt/γ-Al_2O_3 oxidation (mesh size of 40–50). C_0 = 600 ppmv. SV = 35,000 h^{-1}.

from complete oxidation of Nap. Fig. 9 depicts the conversation, residual fraction and mineralization of Nap as a function of temperature. Over 90% of mineralization can be achieved at the moderate reaction temperature of 500 K and at a space velocity of 35,000 h^{-1}. Relative to the temperature of conversion of 90% Nap (470 K), there is about 30 K delay. The reason of the delay of temperature may be due to the production of intermediates or byproducts, which may need to be further oxidized to CO_2. The destruction of Nap may thus generate intermediates or byproducts as secondary pollutants. These intermediates will need to be further identified. Regarding the temperatures at various mineralizations of 10 ($M_{10\%}$), 50 ($M_{50\%}$) and 90 ($M_{90\%}$), the results of this study are about 468, 480 and 500 K, respectively, being lower than 506, 540 and 566 K reported by Zhang et al. [19].

3.4. Chemical reaction kinetics of oxidation of naphthalene over Pt/γ-Al_2O_3

Referring to the catalytic oxidation of *N*,*N*-dimethylformamide [33], we may describe the oxidation kinetics of Nap over Pt/γ-Al_2O_3 catalyst using Rideal–Eley (RE) mechanism [25,33]. The catalytic oxidation of Nap in air is a first-order reaction, yielding

$$-\frac{dC}{dt} = kC \tag{1}$$

where C is the concentration of Nap and k is the apparent rate constant of Nap under catalytic oxidation in air (s^{-1}).

In terms of conversion of Nap (X, $X = (C_{in} - C)/C_{in}$), Eq. (1) becomes

$$\frac{dX}{dt} = -\frac{d(C/C_{in})}{dt} = k(1 - X) \tag{2}$$

Fig. 10 illustrates the plot of $\ln(1 - X)$ versus t at various reaction temperatures for the catalytic oxidation over Pt/γ-Al_2O_3 catalyst with the correlation coefficient, R^2, in the range of 0.9839–0.9921. Because the data presented here are average values, R^2 is thus estimated according to these values. The results indicate a straight-line relationship between $\ln(1 - X)$ and t, supporting that the assumption of first-order reaction is reasonable. This is represented by

$$-\ln(1 - X) = kt \tag{3}$$

where t is the space time (s).

The so-called space time, t, is defined as the reciprocal of the space velocity. A straight line plot of $\ln(1 - X)$ versus t yields the slope of k.

According to the Arrhenius equation, the reaction rate constant (k) can be described as follows:

$$\ln k = \ln A - \frac{E}{R_G T} \tag{4}$$

where A, E, R_G and T are the frequency factor, activation energy, ideal gas law constant and absolute temperature, respectively.

Fig. 11 presents the Arrhenius plots for the catalytic oxidation of Nap over Pt/γ-Al_2O_3 catalyst. A linear plot is obtained with the correlation coefficient (R^2) of 0.9994. Table 3 summarizes the kinetic parameters obtained from the analysis. Substituting these kinetic parameters into Eq. (3), we can reconstruct the performance curves of X versus T in Fig. 8, where space velocity is the reciprocal of space time. The activation energy and frequency factor are 149.97 kJ/mol (35.4 kcal/mol) and 3.26×10^{17} s^{-1}, respectively.

Jess [39] pointed out that the activation energy and frequency factor were 350 kJ/mol and 1.7×10^{14} s^{-1} of the thermal oxidation of Nap, respectively. It is obvious that the oxidation of Nap over Pt/Al_2O_3 can largely decrease the activation energy. To the best of our knowledge, the reaction kinetics of oxidation of Nap over Pt/γ-Al_2O_3 catalyst has not been reported. However, Li and Chen [20] studied the influence of Pt on the catalytic activity of Ni/Al_2O_3 in the investigation of steam reforming by using Nap as a model compound. Their results of reactions kinetics calculation showed that, on Ni-0.05 wt.% Pt/Al_2O_3, the reaction orders

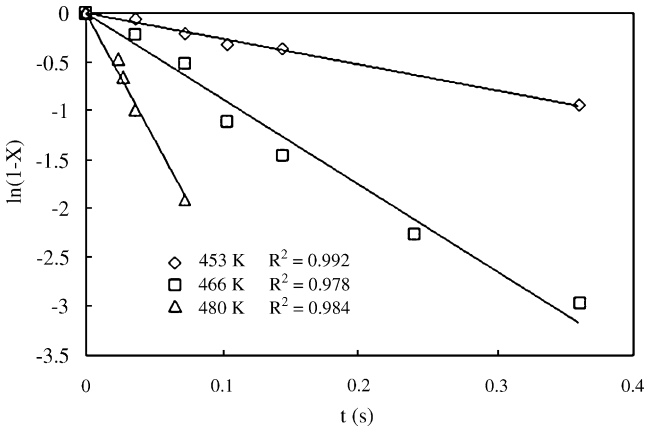

Fig. 10. Plots of $\ln(1 - X)$ vs. space time (t) at various temperatures using Pt/γ-Al_2O_3 catalyst of mesh size 40–50. $C_0 = 600$ ppmv.

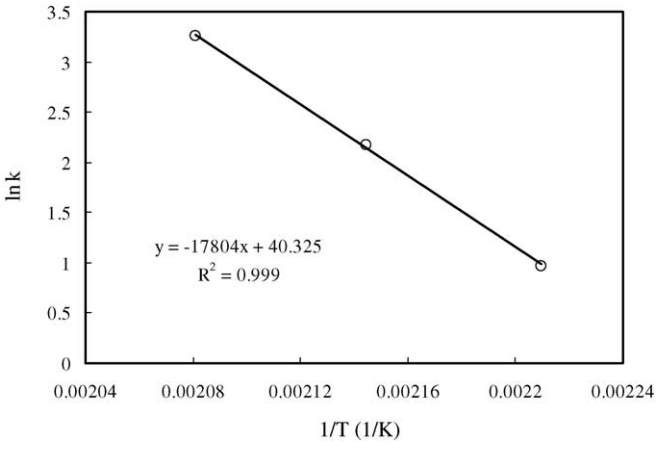

Fig. 11. Arrhenius plot of reaction rate constants for Nap via oxidation using Pt/γ-Al_2O_3 catalyst of mesh size 40–50.

Table 3
Reaction rate constants and activation energy for the catalytic oxidation of naphthalene at various temperatures as computed by the Arrhenius rate equation[a]

Temperature (K)	Reaction rate constant (s^{-1})	R^2	Activation energy (kJ/mol)	Frequency factor (s^{-1})
453	2.63	0.992	149.97 ($R^2 = 0.999$)	3.26×10^{17}
466	8.79	0.978		
480	25.89	0.984		

[a] Computation of constants is based on a linear least squares analysis of a global first-order model for catalytic decomposition in an isothermal tubular fixed-bed reactor.

of Nap and steam are 0.88 and 1.26, while the activation energy and the frequency factor are 262.3 kJ/mol (62.75 kcal/mol) and $3.53 \times 10^{15} s^{-1}$, respectively. The activation energy reported by Li and Chen [20] is higher than that of sole Pt/Al_2O_3 catalyst used in this study. However, less carbon-deposit and fewer types of organic by-products were found on the Ni-0.1 wt.% Pt/Al_2O_3 than on the Ni/Al_2O_3. As for the oxidation of other VOCs by using Pt/Al_2O_3 catalyst, the activation energies of *N*,*N*-dimethyl-formamide, cyclopentane, methane, *n*-hexane and toluene were reported as 48.9 [33], 46, 75.2 [40], 94 and 73 kJ/mol [41], respectively. Further studies will be helpful to develop the reaction rates in terms of coverage, structure of the molecule and molecular weight. For the oxidation of other VOCs by using other Pt catalysts, the activation energy of methane and propane were reported as 21.4 kJ/mol (Pt/SiO_2) [42] and 87.4–115.9 kJ/mol (Pt/glass fiber) [43], respectively. Obviously, the activation energies for other VOCs are all lower than those of Nap by using $Pt/\gamma\text{-}Al_2O_3$. It appears that Nap is a refractory compound to be decomposed although it can be satisfactorily destroyed by certain catalysts, e.g., $Pt/\gamma\text{-}Al_2O_3$ catalyst. The kinetic parameters and mechanism proposed in this study describe the destruction of Nap via combustion. The information is useful for engineering combustion systems of Nap. The kinetics of formation of intermediates or carbon dioxide needs to be further identified. For the scaling-up of the process, it needs to consider the effects caused by mass transfer as well as heat transfer in a large-scale system. However, the kinetics proposed by this study is intrinsic and can be applied for the large-scale system.

4. Conclusions

The catalytic oxidation of naphthalene using a $Pt/\gamma\text{-}Al_2O_3$ catalyst is conducted at various operating conditions. The results indicate that the $Pt/\gamma\text{-}Al_2O_3$ catalyst used accelerates the reaction rate of decomposition of Nap and decreases the reaction temperature as the space velocity decreases. A high conversion (over 95%) can be achieved at moderate reaction temperature of 480 K and space velocity below 35,000 h^{-1}. The reaction temperature needed to exceed 1000 K to achieve conversions over 95% for the case without $Pt/\gamma\text{-}Al_2O_3$ catalyst. The results of the kinetic study indicate that the Rideal–Eley mechanism and Arrhenius equation can be applied to describe the experimental data by using the pseudo-first-order reaction kinetic equation. The activation energy (149.97 kJ/mol) and frequency factor (3.26×10^{17} s^{-1}) are obtained.

Acknowledgement

We express our sincere thanks to the National Science Council of Taiwan for the financial support, under the contract number NSC92-2211-E-002-033.

References

[1] International Programme on Chemical Safety (IPCS), Environmental Health Criteria 2002, Selected Non-heterocyclic Polycyclic Aromatic Hydrocarbons, WHO, Geneva, 1998.
[2] R. Preuss, J. Angerer, H. Drexler, Int. Arch. Occup. Environ. Health 76 (2003) 556.
[3] National Toxicology Program (NTP), Toxicology and Carcinogenesis Studies of Naphthalene (CAS no. 91-20-3) in F344/N Rats (Inhalation Studies), Technical Report Series No. 91-20-3, NIH Publication no. 01-4434, US Department of Health and Human Services, Public Health Service, National Institutes of Health, Research Triangle Park NC, USA, 2000.
[4] S. Coons, M. Byrne, M. Goyer, An Exposure and Risk Assessment for Benzo(a)pyrene and Other Polycyclic Aromatic Hydrocarbons: vol. II. Naphthalene, Final Draft Report, USEPA, Office of Water Regulations and Standards, Washington, DC, 1982.
[5] G.C. Koltsakis, A.M. Stamatelos, Prog. Energy Combust. Sci. 23 (1997) 1.
[6] T. Inui, T. Otawa, Appl. Catal. 14 (1985) 83.
[7] U. Hoffmann, T. Rieckmann, Chem. Eng. Technol. 17 (1994) 146.
[8] P. Zelenka, W. Cartellieri, P. Herzog, Appl. Catal. B 10 (1996) 3.
[9] H. Li, C.D. Banner, G.G. Mason, R.N. Westerholm, J.J. Rafter, Atmos. Environ. 30 (1996) 3537.
[10] W.O. Siegl, R.H. Hammerle, H.M. Herrmann, B.W. Wenclawiak, B. Luers-Jongen, Atmos. Environ. 33 (1999) 797.
[11] H. Li, R. Westerholm, J. Chromatogr. A 664 (1994) 177.
[12] P.P. Fu, D. Herreno-Saenz, Environ. Carcinog. Ecotoxicol. Rev. C 17 (1999) 1.
[13] G. Chen, K.A. Strevett, B.A. Vanegas, Biodegration 12 (2001) 433.
[14] H.L. Huang, W.M. Lee, J. Environ. Eng., ASCE 128 (2002) 60.
[15] S.Y. Lee, S.J. Kim, Appl. Clay Sci. 22 (2002) 55.
[16] W. Cooper, M.G. Nickelsen, R.V. Green, S.P. Mezyk, Radiat. Phys. Chem. 65 (4–5) (2002) 571.
[17] B. Legube, S. Guyon, H. Sugimitsu, M. Dore, Water Res. 20 (1986) 197.
[18] Y.H. Chen, C.Y. Chang, S.F. Huang, C.Y. Chiu, D. Ji, N.C. Shang, Y.H. Yu, P.C. Chiang, Y. Ku, J.N. Chen, Water Res. 36 (2002) 4144.
[19] X.W. Zhang, S.C. Shen, L.E. Yu, S. Kawi, K. Hidajat, K.Y.S. Ng, Appl. Catal. A: Gen. 250 (2003) 341.
[20] Z.X. Li, X.R. Chen, Chin. J. Catal. 24 (2003) 253.

[21] A.K. Neyestanaki, L.E. Lindfors, Fuel 77 (1998) 1727.
[22] K.M. Reddy, C. Song, Catal. Today 31 (1996) 137.
[23] R. Weber, T. Sakurai, H. Hagenmaier, Appl. Catal. B: Environ. 20 (1999) 249.
[24] R. Weber, T. Sakurai, Appl. Catal. B: Environ. 34 (2001) 113.
[25] K. Everaert, J. Baeyens, J. Hazard Mater. B109 (2004) 113.
[26] K. Everaert, M. Mathieu, J. Baeyens, E. Vansent, J. Chem. Technol. Biotechnol. 78 (2003) 167.
[27] A. Brückner, M. Baerns, Appl. Catal. A: Gen. 157 (1997) 311.
[28] F. Klingstedt, A. Kalantar Neyestanaki, R. Byggningsbacka, L.-E. Lindfors, M. Lunděn, M. Petersson, P. Tengstrőm, T. Ollonquist, J. Väyrynen, Appl. Catal. A: Gen. 209 (2001) 301.
[29] F. Klingstedt, H. Karhu, A. Kalantar Neyestanaki, L.-E. Lindfors, T. Salmi, J. Väyrynen, J. Catal. 206 (2002) 248.
[30] F. Klingstedt, A. Kalantar Neyestanaki, L.-E. Lindfors, T. Salmi, T. Heikkilä, E. Laine, Appl. Catal. A: Gen. 239 (2003) 229.
[31] S.K. Anderson, J.J. Spivey, Appl. Catal. A: Gen. 81 (1961) 239.
[32] C.J. Heyes, J.G. Irwin, H.A. Johnson, R.L. Moss, J. Chem. Technol. Biotechnol. 32 (1982) 1025.
[33] W.T. Tsai, Y.H. Chang, C.Y. Chang, J. Hazard Mater. 37 (1994) 241.
[34] S.J. Gregg, K.S.W. Sing, Adsorption, Surface and Porosity, second ed. Academic Press, London, 1982.
[35] R.J. Farrauto, C.H. Bartholomew, Fundamentals of Industrial Catalytic Processes, Blankie Academic & Professional, London, 1997, p. 58.
[36] J. Carnö, M. Berg, S. Järås, Fuel 75 (1996) 959.
[37] M. Ferrandon, J. Carnö, S. Järås, E. Björnbom, Appl. Catal. A: Gen. 180 (1999) 153.
[38] C.N. Satterfield, Heterogeneous Catalysis in Industrial Practice, second ed. McGraw-Hill, New York, NY, 1991.
[39] A. Jess, Fuel 75 (1996) 1441.
[40] T.F. Garetto, C.R. Apesteguía, Catal. Today 62 (2000) 189.
[41] N. Radic, B. Grbic, A. Terlecki-Baricevic, Appl. Catal. B: Environ. 50 (2004) 153.
[42] B. Burch, A. Ramli, Appl. Catal. B: Environ. 15 (1998) 63.
[43] L. Kiwi-Minsker, I. Yuranov, E. Slavinskaia, V. Zaikovskii, A. Renken, Catal. Today 59 (2000) 61.